energies

MDPI

Article

Effect of Hydration under High Temperature and Pressure on the Stress Thresholds of Shale

Jianfa Wu [1], Yintong Guo [2], Haoyong Huang [1,*], Guokai Zhao [3], Qiyong Gou [1], Junchuan Gui [1] and Ersi Xu [1]

[1] Shale Gas Research Institute of PetroChina Southwest Oil & Gas Field Company, Chengdu 610051, China; wu_jianfa@petrochina.com.cn (J.W.); gouqiyong@petrochina.com.cn (Q.G.); guijunchuan@petrochina.com.cn (J.G.); xuersi@petrochina.com.cn (E.X.)
[2] State Key Laboratory of Geomechanics and Geotechnical Engineering, Institute of Rock and Soil Mechanics, Chinese Academy of Sciences, Wuhan 430071, China; ytguo@whrsm.ac.cn
[3] State Key Laboratory of Coal Mine Disaster Dynamics and Control, Chongqing University, Chongqing 400044, China; fy1142406117@foxmail.com
* Correspondence: huang_hy@petrochina.com.cn

Abstract: The stress threshold of deep reservoir shale subjected to fracturing fluid immersion is an important factor affecting fracture initiation and propagation during fracturing. However, little information has been reported on the effect on shale of soaking at high temperature and high pressure (HTHP). In this study, immersion tests and triaxial compression tests were carried out at reservoir temperature and in-situ stress on the downhole cores with different mineral compositions. The characteristics of stress thresholds, i.e., crack initiation stress (σ_{ci}), crack damage stress (σ_{cd}), and peak deviator stress (σ_p), of shale affected by the different times of soaking with low-viscosity fracturing fluid (a) and the different viscosity fracturing fluids (a, b, and c) were investigated. The results show that hydration at HTHP has a significant softening effect on the stress thresholds (σ_{ci}, σ_{cd}, σ_p) of reservoir shale, but the softening rate varies for samples with different mineral compositions. The crack initiation stresses of quartz-rich and clay-rich shales treated with different soaking times and different soaking media remain almost unchanged in the range of 47 to 54% of the corresponding peak strength, while the crack initiation stresses of carbonate-rich shales are significantly affected. The ratio σ_{cd}/σ_p of quartz-rich shale is significantly affected by the different viscosity fracturing fluids (a, b) and the different times of soaking with low-viscosity fracturing fluid (a), while clay- and carbonate-rich shales are less affected. The results of this study can provide a reference for the fracturing design of deep shale gas development.

Keywords: shale; stress thresholds; fracturing fluid; high temperature and pressure

Citation: Wu, J.; Guo, Y.; Huang, H.; Zhao, G.; Gou, Q.; Gui, J.; Xu, E. Effect of Hydration under High Temperature and Pressure on the Stress Thresholds of Shale. *Energies* **2023**, *16*, 7778. https://doi.org/10.3390/en16237778

Academic Editors: Manoj Khandelwal, Chun Zhu, Gan Feng and Gan Li

Received: 17 October 2023
Revised: 21 November 2023
Accepted: 24 November 2023
Published: 26 November 2023

1. Introduction

Hydraulic fracturing is the key technology for the efficient development of shale gas [1–3]. During field fracturing, natural fractures and weak planes of bedding are communicated through the segmented multi-cluster perforation and injection of low-viscosity fracturing fluid with a large fluid volume, forming a fracturing network of interlaced natural fractures and artificial fractures, thus increasing the volume of reservoir reconstruction [4,5]. In deep shale reservoirs in the Sichuan Basin of China, the flowback rate of fracturing fluid is generally lower than 30%, indicating that fracturing fluid is often present in the reservoir and cannot be completely recovered in time [6]. In the development of deep shale gas, the selection and use of fracturing fluids often vary depending on the different fracturing conditions in the fracturing design [7]. When low-viscosity fracturing fluid is used, the pressure at the end of the natural fracture makes it easier to reach the threshold of the fracturing pressure, and the fluid pressure is easier to spread in the natural fracture. In order to reduce the percolation of fracturing fluid into the formation during fracturing, high-viscosity fracturing fluid is usually used, which also results in the complexity of

fractures being reduced [8]. However, the effect of thermos-hydro-mechano-chemical (THMC) coupling on fracture propagation of reservoir shale is rarely reported. Therefore, it is necessary to study the effects of fracturing fluid type, viscosity, and immersion time on crack initiation and propagation of shale with different mineral compositions.

Most of the existing studies on hydration effects have been conducted in immersion tests at room temperature and atmospheric pressure [9–15]. Ma et al. showed that the hydration effect on the shale is greatest at the beginning of soaking, and the damage rate decreased as the soaking time increased [16]. Yang et al. showed that the content and type of clay minerals, especially montmorillonite and inter-stratified illite–smectite, have an important effect on the swelling absorption capacity of shales [17]. Tan et al. quantified the effect of different fracturing fluids and shale interactions on the surface roughness of shale fractures [18]. At present, few efforts have been made to study the influence of the immersion of fracturing fluid and flowback fluid that has not been flowback under HTHP on the stress thresholds of reservoir rocks. In order to simulate in-situ conditions that are more in line with deep reservoirs, an experimental study of immersion at HTHP, which has not been widely explored, was conducted in this study.

From the viewpoint of rock mechanics, the stress thresholds of shale under THMC coupling, i.e., crack initiation stress (σ_{ci}), crack damage stress (σ_{cd}), and peak deviator stress (σ_{p}), are important factors affecting crack initiation and propagation in deep shale reservoirs during fracturing [19–22]. Most of the current studies have focused on the influence of confining pressure or bedding effects on the specific stress thresholds of shale at lower confining pressure (uniaxial or confining pressure lower than 50 MPa) [23–25]. However, there are few studies on the influence of the hydration effect under HTHP on the characteristic stress of reservoir rocks, although it is of great engineering importance for deep shale gas development.

In this study, the indoor immersion tests and mechanical tests under HTHP were conducted on reservoir shales collected from three different sublayers of the Wufeng-Longmaxi Formation in the Luzhou block, focusing on the influence of different soaking times and media on the specific stress thresholds of the reservoir rock. The crack initiation stress and crack damage stress were obtained by analysis of the axial strain–crack volumetric strain and the axial strain–volumetric strain curves, with the aim of investigating the variation of specific stress thresholds of downhole cores interact with the low-viscosity fracturing fluid (a) commonly used in fracturing sites for different soaking times (0 h, 2 h, 3 days, 15 days). Additionally, the effect of different fracturing fluids (a, b, and c) on the specific stress threshold of shale at the same soaking time of 3 days was investigated. The effects of different soaking times of low-viscosity fracturing fluid immersion and different immersion media (a, b, c) on the crack initiation stress and crack damage stress of shale specimens are revealed, which can deepen the understanding of the crack initiation and propagation mechanism of THMC-treated shales with different mineral compositions.

2. Test Materials and Procedures

2.1. Sample

The shale used in the test was collected from the deep reservoir of the Wufeng–Longmaxi Formation in the Luzhou block of the southern Sichuan Basin, China, at a vertical depth of 4009.30–4091.60 m. To investigate the effect of soaking at HTHP on the specific stress thresholds of shales with different mineral compositions, full-diameter cores with typical mineral composition percentages were collected, and the mineralogical composition test results are detailed in Figure 1. The studied samples were categorized into three groups, i.e., clay-rich (32.3%) L1–4 shale, quartz-rich (59.6%) L1–2 shale, and carbonate-rich (42.1%) WF shale. A total of 36 standard cylindrical samples, 25 mm diameter by 50 mm height, were produced from the full-diameter core of each layer along parallel bedding orientations using a waterless wire-cutting method, as shown in Figure 2. Subsequently, samples with a polished end face nonparallelism less than 0.02 mm were

used for immersion and mechanical testing under HTHP. Figure 3 illustrates the work steps in the form of a flowchart.

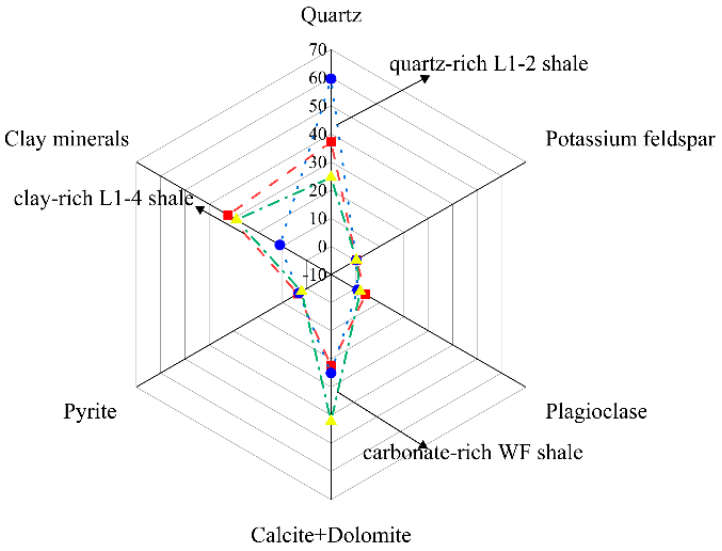

Figure 1. Mineral composition of the studied shale.

Figure 2. Photographs of samples used for testing.

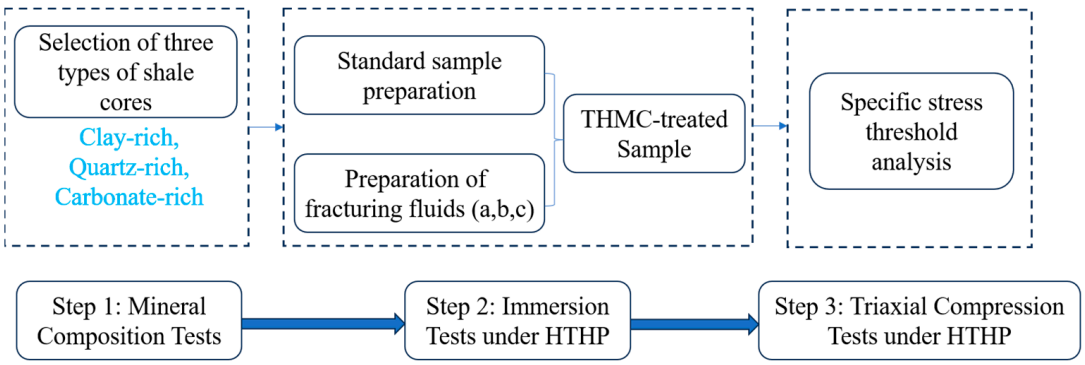

Figure 3. Workflow of experimental research.

2.2. Preparation of the Fracturing Fluid

In this study, the simulated fracturing fluids used in the laboratory soaking test were three kinds of fracturing fluids commonly used in field fracturing operations in the Luzhou block, i.e., low-viscosity soaking medium (a) with a viscosity of 3 mPa·s prepared by

friction reducer and deionized water, high-viscosity soaking medium (b) with a viscosity of 50 mPa·s prepared by friction reducer and deionized water, and low-viscosity soaking medium (c) with a viscosity of 3 mPa·s prepared by friction reducer and flowback fluid. The difference between soaking media (a) and (c) is that, as shown in the study of Hu et al. [26], the type and concentration of ions in the flowback fluid and the injected fracturing fluid are significantly different. Three types of fracturing fluids were used to study the following fracturing field concerns. One of them is the evolution of stress thresholds and failure modes with soaking time for the interaction of low-viscosity fracturing fluid (a) with downhole cores of different mineral compositions. The second one compares the effect of different types of fracturing fluids (a, b, c) on the stress thresholds of shale at the same soaking time of 3 days.

2.3. Test Procedure

First, the soaking media a, b, and c were prepared according to the above requirements. Processed standard samples were placed in a high-temperature and high-pressure immersion chamber containing freshly prepared fracturing fluid, as shown in Figure 4. Subsequently, they were set to the designated temperature and pressure to simulate in-situ formation conditions. The reservoir temperature and pressure conditions corresponding to the vertical depths of 4009.30–4091.60 m, obtained from the temperature and in-situ stress in the logging data, are 130 °C—90 MPa. Since the immersion test under high temperature and high pressure (HTHP) needs to be cooled down to room temperature before unloading the confining pressure, it is not convenient to stop the test at any time. In this study, the soaking time was recorded starting after the temperature was elevated at a rate of 5 °C/min to 130 °C to reach stability. The samples were prepared with fracturing fluid and soaking medium (a) under HTHP for 2 h, 3 days, and 15 days, respectively. After the designated soaking time is reached, the heating is stopped and the cooling down to room temperature is started at a rate of approximately 5 °C/min. Finally, the samples were removed from the reaction chamber and dried before conducting the subsequent triaxial compression tests at reservoir temperature and pressure. It should be noted that the actual immersion time here refers to the duration between the heating to the designated temperature of 130 °C and turning off the heating device. Using MTS 815 testing system, triaxial compression tests were conducted on THMC-treated downhole cores at a loading rate of 0.06 mm/min under in-situ reservoir temperature and pressure (T = 130 °C, Pc = 90 MPa).

Figure 4. Fluid–rock reactor at high temperature and pressure.

In addition, to investigate the effects of different soaking media (a, b, and c) on the specific stress thresholds of shale, soaking tests and mechanical tests on downhole cores

interacting with three soaking media at 3 days at HTHP were conducted using the methods described above.

2.4. Determination of the Stress Thresholds

In the current research, significant progress has been made in studies related to specific stress thresholds (e.g., crack closure stress, crack initiation stress, crack damage stress) in rocks under uniaxial or lower confining pressure conditions, which are used to guide engineering practice. Since most of the initial microcracks are closed at such high hydrostatic pressures in the deep formation, the closure effect that occurs under external loading at lower confining pressures is relatively less important in the case of high confining pressure conditions. The crack initiation stress refers to the critical strength at which cracks begin to sprout within the rock, i.e., the onset of stable crack expansion. The crack damage stress refers to the critical strength at which cracks enter unstable expansion, marking the massive penetration of cracks within the rock and the deflection of the volumetric strain curve. The study of characteristic stress threshold can provide valuable data reference for the evolution and fracture mechanism of microcracks in samples. However, the effect of immersion under HTHP on the specific stress thresholds of shale remains understudied in this regard.

Although extensive research has been conducted on how to determine these two stress thresholds, a unified recommended method for determining crack initiation stress and crack damage stress has not been developed. The methods can be divided into the following five categories: acoustic emission method [27], crack–strain method [28], lateral strain method [29], volumetric strain method [30], and moving point regression determination method [25]. Since shale is a brittle and hard sedimentary rock, the number of acoustic emission events during triaxial compression tests is very small, reaching a maximum only at the moment close to failure, so the acoustic emission method is not applicable to the determination of characteristic stresses in brittle and hard rocks such as shale. The physical significance of the crack–strain model calculation method is clear and allows for easy and accurate determination of crack initiation stresses and damage stresses in rocks. The crack–strain model was first proposed by Cai et al. [31] and the crack initiation stress and crack damage stress of rocks were calculated using this model method, and it has been widely used.

The method for determining the shale crack initiation stress and crack damage stress is shown in Figure 5. The volumetric strain of the rock is assumed to consist of elastic volumetric strain (ε_{eV}) and crack volumetric strain (ε_{cV}), as shown in the following equation.

$$\varepsilon_V = \varepsilon_{eV} + \varepsilon_{cV} = \varepsilon_1 + 2\varepsilon_3 \tag{1}$$

where ε_1, ε_3 are the axial and circumferential strains of the samples tested in the triaxial compression test, respectively.

According to the generalized Hooke's law:

$$\varepsilon_1^e = \frac{1}{E}[\sigma_1 - \mu(\sigma_2 + \sigma_3)] \tag{2}$$

$$\varepsilon_2^e = \frac{1}{E}[\sigma_2 - \mu(\sigma_1 + \sigma_3)] \tag{3}$$

$$\varepsilon_3^e = \frac{1}{E}[\sigma_3 - \mu(\sigma_1 + \sigma_2)] \tag{4}$$

where, E is the elastic modulus, μ is Poisson's ratio, σ_1 is the axial principal stress, $\sigma_2 = \sigma_3$ is the confining pressure.

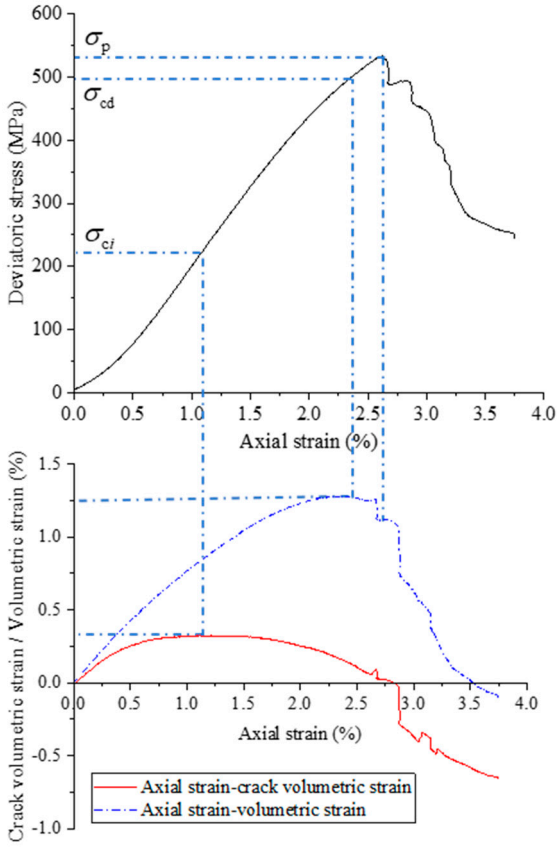

Figure 5. Schematic diagram of the crack initiation stress (σ_{ci}), crack damage stress (σ_{cd}), and peak deviator stress (σ_p).

The elastic volumetric strain is as follows:

$$\varepsilon_{eV} = \varepsilon_1^e + \varepsilon_2^e + \varepsilon_3^e = \frac{1-2\mu}{E}(\sigma_1 - \sigma_3) \quad (5)$$

The crack volumetric strain is as follows:

$$\varepsilon_{cV} = \varepsilon_1 + 2\varepsilon_3 - \frac{1-2\mu}{E}(\sigma_1 - \sigma_3) \quad (6)$$

As shown in Figure 5, the corresponding stresses at the inversion points of the axial strain–crack volumetric strain and the axial strain–volumetric strain curves are the crack initiation stress and the crack damage stress, respectively. The extreme values of the crack volumetric strain and total volumetric strain can be easily obtained from the experimental data. However, the axial strain–crack volumetric strain as well as the axial strain–volumetric strain curves vary very smoothly at the inversion points.

3. Results and Discussion

3.1. Stress–Strain Curve

Figure 6 shows the typical stress–strain curves for each sublayer of cores under different soaking times (0 h, 2 h, 3 days and 15 days) of the interaction between soaking fluid a and shale, and under the interaction with different soaking media a, b, c at the same immersion time of 3 days. In fluid–shale interaction under HTHP, the stress–strain response of the clay-rich L1–4 shale is more obviously affected by immersion, which shows a significant decrease in peak deviatoric stress and elastic modulus. The stress–strain response of the clay-rich L1–4 shale is most significantly affected by the hydration effect when the shale interacted with the soaking media a, b for 3 days, while the interaction with the soaking medium c has little effect on the shale. The effect of hydration on the stress–

strain relationship of the carbonate-rich WF shale is slightly inferior to that on the clay-rich shale, showing a lower magnitude of peak strength and elastic modulus deterioration. The behavior of the WF shale is more obviously influenced by the hydration effect under HTHP when soaked with soaking medium a for 3 days. The weakest effect is on the quartz-rich L1–2 shale when the soaking time is lower than 15 days in the laboratory test conditions of this study.

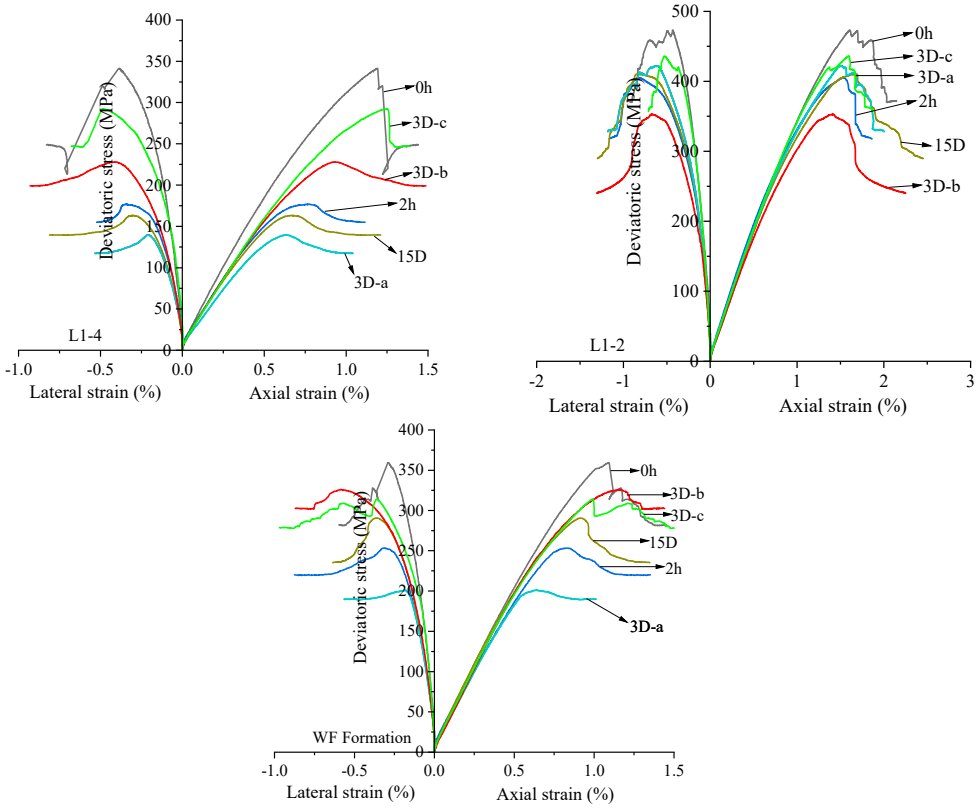

Figure 6. Typical stress–strain curves of cores from each sublayer immersed under HTHP (h, hours; D, days).

Overall, the effect of fracturing fluid–shale interaction on the stress–strain response of shale under HTHP is as follows in descending order: clay-rich L1–4 shale > carbonate-rich WF shale > quartz-rich L1–2 shale.

3.2. Characteristics of Stress Thresholds

Figure 7 illustrates the evolution of stress thresholds (σ_{ci}, σ_{cd}, σ_p) of shales with different mineral compositions as the fracturing fluid–shale interaction proceeds. It can be seen that the strength parameters of the three types of shale samples decrease rapidly after soaking for 2 h. Overall, the strength parameters show a decreasing trend as soaking proceeds, except for the 15-day soaking cases in the L1–4 and WF shales. It indicates that hydration at HTHP has a significant softening effect on the mechanical performance of the reservoir shale, but the softening rate varies for samples with different mineral compositions. For the L1–4 and WF shales, the strength initially decreases and then increases with increasing soaking time, reaching a minimum strength at 3 days. Note that after 15 days of immersion treatment, the strength, although improved, was still lower than the strength without immersion. The peak strength of the L1–2 shale decreased rapidly after 0 ~ 2 h of soaking treatment, whereas hydration had little effect on strength after 2 ~ 3 d of immersion.

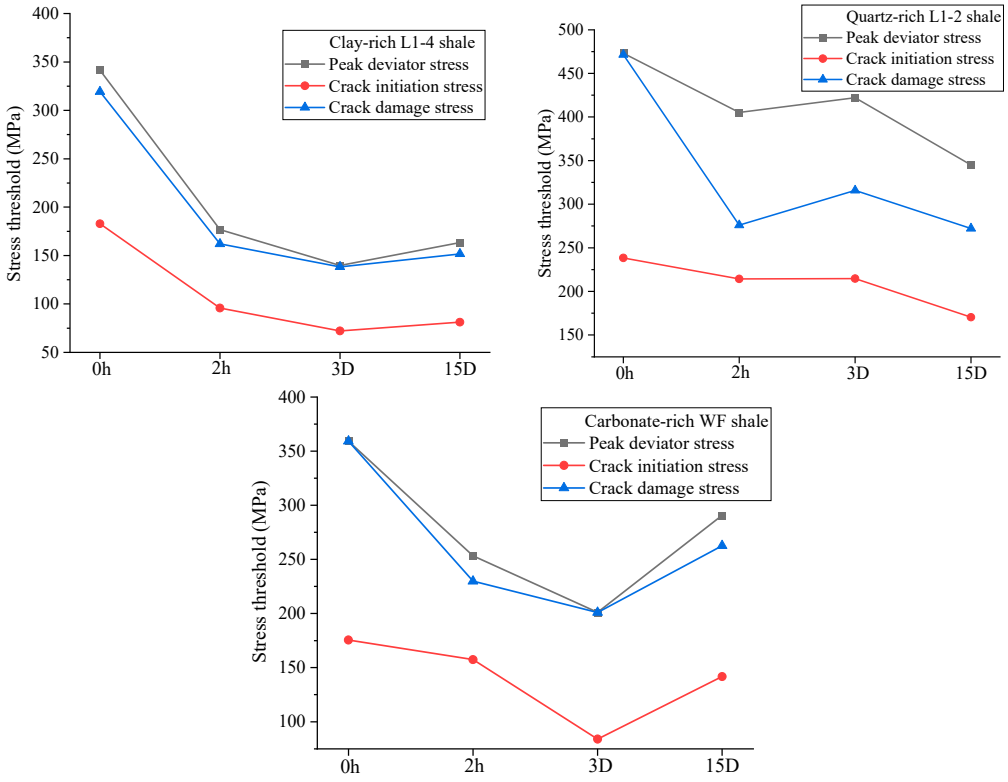

Figure 7. Variation of stress thresholds (crack initiation stress, crack damage stress, peak strength) (h, hours; D, days).

To study the effect of the different times of soaking with low-viscosity fracturing fluid (a) on stress thresholds of shale under HTHP, the equations are characterized as follows:

$$k_{\sigma_{ci}} = 1 - \frac{\sigma_{ci-t}}{\sigma_{ci-0}} \quad (7)$$

$$k_{\sigma_{cd}} = 1 - \frac{\sigma_{cd-t}}{\sigma_{cd-0}} \quad (8)$$

$$k_{\sigma_{p}} = 1 - \frac{\sigma_{p-t}}{\sigma_{p-0}} \quad (9)$$

where, $k_{\sigma_{ci}}$, $k_{\sigma_{cd}}$, and $k_{\sigma_{p}}$ are indices of the effects of different soaking times on the crack initiation stress, crack damage stress, and peak deviator stress of shale, respectively. σ_{ci-t}, σ_{cd-t}, and σ_{p-t} are the crack initiation stress, crack damage stress, and peak deviator stress at different soaking times (t = 2 h, 3 days, 15 days), respectively. σ_{ci-0}, σ_{cd-0}, and σ_{p-0} are the values without soaking treatment, respectively.

For L1–4 clay-rich shale, the effects of hydration on stress thresholds (σ_{ci}, σ_{cd}, σ_{p}) are in the range of 48.23 to 59.08%, 47.65 to 60.54%, and 51.44 to 58.75%, respectively. The influence on the carbonate-rich shales of the Wufeng Formation is the next most important, ranging from 19.07~44.00%, 10.32~52.13%, and 26.88~44.05%, respectively. It is noteworthy that hydration has little effect on the crack initiation stress and peak strength of the L1–2 quartz-rich shale in the range of 12%, while the effect on the crack damage stress is larger, in the range of 33.01 to 42.26%.

Figure 8 shows the variation of the stress thresholds of the three types of shale when soaked for 3 days in different soaking media (a, b, and c). Overall, the effect on the stress thresholds of the shales with different mineral compositions when using immersion medium (c) is small, in the range of 20%, indicating that the flowback fluid may have an inhibitory effect on the hydration cracking of the sample. Particularly, the stress thresholds of the quartz-rich shale are less affected by the interaction of fluid c-shale, within 10%.

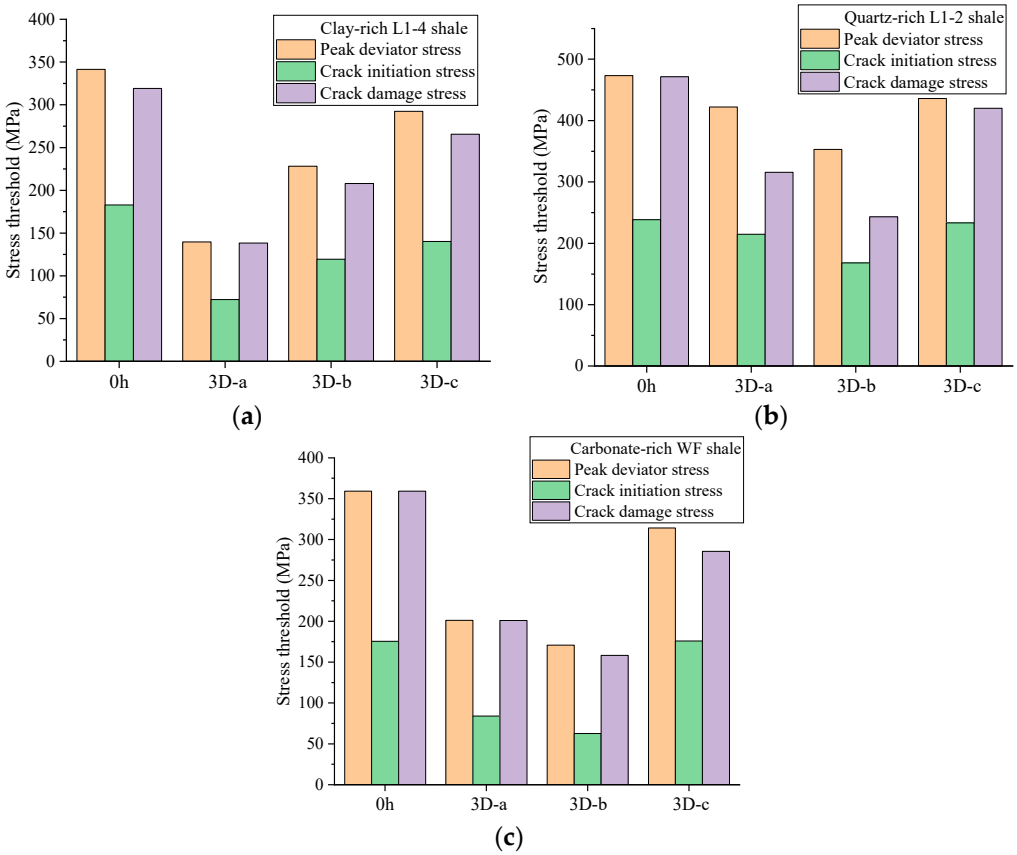

Figure 8. Variation of stress thresholds (crack initiation stress, crack damage stress, peak strength) of shale after interaction with different soaking media (low-viscosity fracturing fluid (**a**) with a viscosity of 3 mPa·s, high-viscosity fracturing fluid (**b**) with a viscosity of 50 mPa·s, and low-viscosity flowback fluid (**c**) with a viscosity of 3 mPa·s).

The effect of low-viscosity fracturing fluids on the crack stress threshold of clay-rich shale is higher than that of high-viscosity fracturing fluids, probably because clay minerals are more likely to produce hydrated fractures when immersed in low-viscosity fracturing fluids, which affects the characteristic stress threshold of the shale.

For quartz-rich L1–2 shale, the effects on both crack initiation stress and peak strength when interacting with immersion media (a) and (c) are less than 5% compared to the unsoaked sample. However, the effect of the two fluid immersions on the crack damage stress differed significantly, 33.01% and 8.8%, respectively. It indicates that water has an important effect on crack unstable crack initiation extension, while the flowback fluid has little effect on it.

3.3. Characteristics of the Relationships between Peak Stress and Crack–Stress Thresholds

Figure 9 depicts the evolution of the ratio of crack initiation stress (σ_{ci}) and crack damage stress (σ_{cd}) to peak deviator stress (σ_p) for the three types of shale at different soaking times. For clay-rich shale and quartz-rich shale, the proportion of σ_{ci}/σ_p ranges from 47% to 54%. Although σ_{ci}/σ_p tends to decrease with increasing soaking time, it only decreases slightly. For carbonate-rich shale, σ_{ci}/σ_p still shows a variation pattern that fluctuates within a certain range with the increase in soaking time, which may be caused by the dissolution and regeneration of carbonate minerals [32,33]. With increasing soaking time, the effect of hydration at HTHP on the internal crack initiation in carbonate-rich shale samples is more significant, while it has little effect on quartz-rich and clay-rich shales.

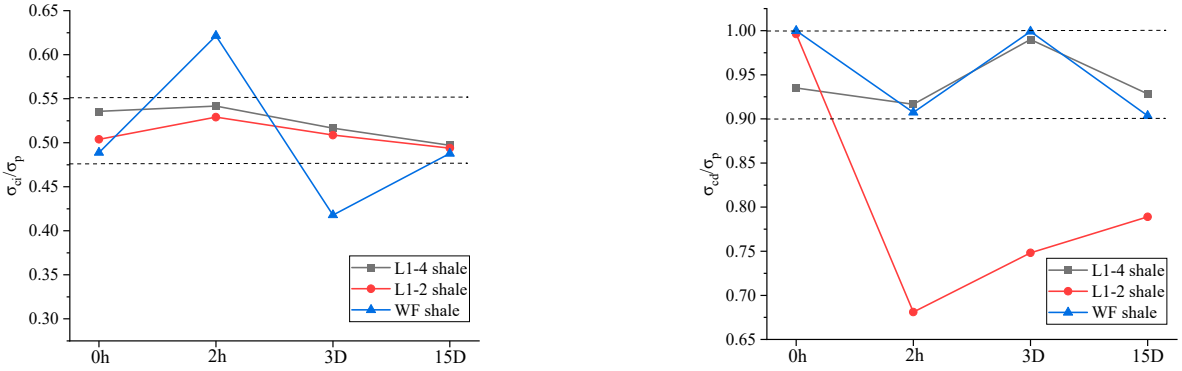

Figure 9. Variation of σ_{ci}/σ_p and σ_{cd}/σ_p cores under reservoir temperature and pressure with increasing soaking time (h, hours; D, days).

The variation of the ratio of crack damage stress to peak deviator stress with soaking time is closely related to the mineral composition of the specimen. For L1–4 and WF shale with obvious hydration cracks after immersion, σ_{cd}/σ_p changes little in the range of 0.9 to 1 before immersion for 15 days, indicating that the presence of hydration cracks may play a suppressive role in the unstable expansion of cracks within the samples. In other words, the sample is more likely to fracture along the hydration crack during the process of deformation and failure. Although the soaking at HTHP appears to have a weak effect on the strength of the quartz-rich shale, it has a greater impact on the crack damage stress threshold.

Figure 10 depicts the ratio of crack initiation stress and crack damage stress to peak strength for the three types of shale immersed in different soaking media (a, b, and c) at the same soaking time of 3 days. As shown in Figure 10, the effects of different fracturing fluids on σ_{ci}/σ_p of both clay-rich and quartz-rich shales are small, while the effect on the ratio of carbonate-rich shale is more significant, which is similar to the effect of different soaking times on the crack initiation stress described above.

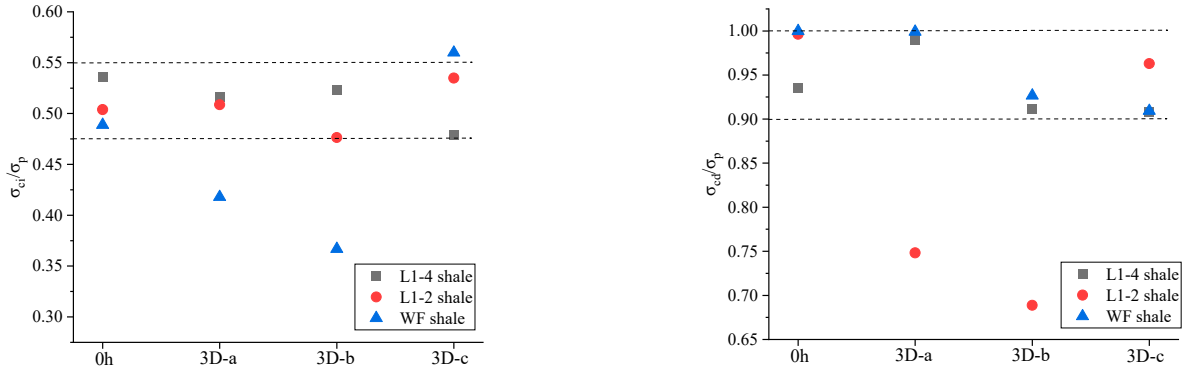

Figure 10. Variation of σ_{ci}/σ_p and σ_{cd}/σ_p of shale after interaction with different soaking media (low-viscosity fracturing fluid (a) with a viscosity of 3 mPa·s, high-viscosity fracturing fluid (b) with a viscosity of 50 mPa·s, and low-viscosity flowback fluid (c) with a viscosity of 3 mPa·s).

The ratio of crack damage stress to peak strength of the samples is significantly reduced by the interaction of the higher viscosity fracturing fluid–shale. However, σ_{cd}/σ_p is not significantly affected by the immersion of flowback fluid, probably because the ionic effect contained in the flowback fluid has an inhibitory effect on the unstable expansion of cracks inside the sample.

In summary, the crack initiation stresses of quartz-rich and clay-rich shales treated with different soaking times and different soaking media remain almost unchanged in the range of 47 to 54% of the corresponding peak strength, while the crack initiation stresses of carbonate-rich shales are significantly affected. The ratio of crack stress thresholds (σ_{ci}, σ_{cd})

to the peak strength of the three types of shale after immersion treatment with flowback fluid (c) changed slightly compared to the unsoaked samples. The ratio of crack damage stress to the corresponding peak strength of quartz-rich shale is significantly affected by the different times of soaking with low-viscosity fracturing fluid (a) and the different viscosity fracturing fluids (a, b). However, σ_{cd}/σ_p of the clay-rich and carbonate-rich shales are not significantly affected by the different viscosity fracturing fluids (a, b) and the different times of soaking with low-viscosity fracturing fluid (a). The lack of microscopic observation of the samples after immersion treatment is also a limitation of this work. Further studies based on μm-CT and SEM techniques will be carried out in future work to investigate the degradation mechanism of shale after THMC treatment.

4. Conclusions

In this study, the effects of different soaking times (0 h, 2 h, 3 days, 15 days) and different soaking media (a, b, c) on the stress thresholds of shale were investigated by soaking tests and triaxial compression tests at 130 °C—90 MPa conditions. The main conclusions are as follows:

(1) Overall, the effect of fracturing fluid–shale interaction on the stress–strain response of shale under HTHP is as follows in descending order: clay-rich L1–4 shale > carbonate-rich WF shale > quartz-rich L1–2 shale.

(2) Hydration at HTHP has a significant softening effect on the stress thresholds of the reservoir shale, i.e., crack initiation stress (σ_{ci}), crack damage stress (σ_{cd}), and peak deviator stress (σ_p), but the softening rate varies for samples with different mineral compositions. The crack initiation stresses of quartz-rich and clay-rich shales treated with different soaking times and different soaking media remain almost unchanged in the range of 47 to 54% of the corresponding peak strength, while the crack initiation stresses of carbonate-rich shales are significantly affected.

(3) The ratio of crack stress thresholds (σ_{ci}, σ_{cd}) to the peak strength of the three types of shale after immersion treatment with flowback fluid (c) changed slightly compared to the unsoaked samples. The ratio of crack damage stress to the corresponding peak strength of quartz-rich shale is significantly affected by the different times of soaking with low-viscosity fracturing fluid (a) and the different viscosity fracturing fluids (a, b). However, σ_{cd}/σ_p of the clay-rich and carbonate-rich shales are not significantly affected by the different viscosity fracturing fluids (a, b) and the different times of soaking with low-viscosity fracturing fluid (a).

Author Contributions: Software, E.X.; Validation, J.G.; Resources, J.W. and H.H.; Data curation, Q.G.; Writing—review & editing, J.W., H.H. and G.Z.; Supervision, Y.G. All authors have read and agreed to the published version of the manuscript.

Funding: This research received no external funding.

Data Availability Statement: The authors are unable or have chosen not to specify which data has been used.

Conflicts of Interest: Authors Jianfa Wu, Haoyoung Huang, Qiyoung Gou, Junchuan Gui and Ersi Xu were employed by PetroChina Southwest Oil & Gas Field Company. All authors declare that the research was conducted in the absence of any commercial or financial relationship that could be constructed as a potential conflict of interest.

References

1. Zhao, J.; Ren, L.; Jiang, T.; Hu, D.; Wu, L.; Wu, J.; Yin, C.; Li, Y.; Hu, Y.; Lin, R.; et al. Ten years of gas shale fracturing in China: Review and prospect. *Nat. Gas Ind. B* **2022**, *9*, 158–175. [CrossRef]
2. Zou, C.; Zhu, R.; Chen, Z.-Q.; Ogg, J.G.; Wu, S.; Dong, D.; Qiu, Z.; Wang, Y.; Wang, L.; Lin, S.; et al. Organic-matter-rich shales of China. *Earth Sci. Rev.* **2019**, *189*, 51–78. [CrossRef]
3. Zhao, G.; Guo, Y.; Yang, C.; Wang, L.; Guo, W.; Yang, H.; Wu, X.; Liu, H. Anisotropic mechanical behavior of ultra-deep shale under high in-situ stress, a case study in the Luzhou block of the southern Sichuan Basin, China. *Int. J. Rock Mech. Min. Sci.* **2023**, *170*, 105536. [CrossRef]

4. Hou, B.; Chen, M.; Cheng, W.; Diao, C. Investigation of Hydraulic Fracture Networks in Shale Gas Reservoirs with Random Fractures. *Arab. J. Sci. Eng.* **2016**, *41*, 2681–2691. [CrossRef]
5. Zhao, G.; Guo, Y.; Chang, X.; Jin, P.; Hu, Y. Effects of temperature and increasing amplitude cyclic loading on the mechanical properties and energy characteristics of granite. *Bull. Eng. Geol. Environ.* **2022**, *81*, 155. [CrossRef]
6. Bai, J.; Kang, Y.; Chen, Z.; You, L.; Chen, M.; Li, X. Changes in retained fracturing fluid properties and their effect on shale mechanical properties. *J. Nat. Gas Sci. Eng.* **2020**, *75*, 103163. [CrossRef]
7. You, L.; Zhou, Y.; Kang, Y.; Yang, B.; Cui, Z.; Cheng, Q. Fracturing fluid retention in shale gas reservoirs:mechanisms and functions. *Arab. J. Geosci.* **2019**, *12*, 1–17. [CrossRef]
8. Yan, X.; Kang, Y.; You, L.; Xu, C.; Lin, C.; Zhang, J. Drill-in fluid loss mechanisms in brittle gas shale: A case study in the Longmaxi Formation, Sichuan Basin, China. *J. Pet. Sci. Eng.* **2019**, *174*, 394–405. [CrossRef]
9. Zhang, W.; Zhang, D.; Zhao, J. Experimental investigation of water sensitivity effects on microscale mechanical behavior of shale. *Int. J. Rock Mech. Min. Sci.* **2021**, *145*, 104837. [CrossRef]
10. Meng, F.; Ge, H.; Yan, W.; Wang, X.; Wu, S.; Wang, J. Effect of saturated fluid on the failure mode of brittle gas shale. *J. Nat. Gas Sci. Eng.* **2016**, *35*, 624–636. [CrossRef]
11. Zhou, D.; Zhang, G.; Huang, Z.; Zhao, J.; Wang, L.; Qiu, R. Changes in microstructure and mechanical properties of shales exposed to supercritical CO2 and brine. *Int. J. Rock Mech. Min. Sci.* **2022**, *160*, 105228. [CrossRef]
12. Feng, G.; Wang, X.; Kang, Y.; Zhang, Z. Effect of thermal cycling-dependent cracks on physical and mechanical properties of granite for enhanced geothermal system. *Int. J. Rock Mech. Min. Sci.* **2020**, *134*, 104476. [CrossRef]
13. Feng, G.; Wang, X.; Wang, M.; Kang, Y. Experimental investigation of thermal cycling effect on fracture characteristics of granite in a geothermal-energy reservoir. *Eng. Fract. Mech.* **2020**, *235*, 107180. [CrossRef]
14. Feng, G.; Kang, Y.; Wang, X.; Hu, Y.; Li, X. Investigation on the Failure Characteristics and Fracture Classification of Shale Under Brazilian Test Conditions. *Rock Mech. Rock Eng.* **2020**, *53*, 3325–3340. [CrossRef]
15. Feng, G.; Kang, Y.; Sun, Z.-D.; Wang, X.-C.; Hu, Y.-Q. Effects of supercritical CO2 adsorption on the mechanical characteristics and failure mechanisms of shale. *Energy* **2019**, *173*, 870–882. [CrossRef]
16. Ma, T.; Yang, C.; Chen, P.; Wang, X.; Guo, Y. On the damage constitutive model for hydrated shale using CT scanning technology. *J. Nat. Gas Sci. Eng.* **2016**, *28*, 204–214. [CrossRef]
17. Yang, L.; Ge, H.; Shi, X.; Cheng, Y.; Zhang, K.; Chen, H.; Shen, Y.; Zhang, J.; Qu, X. The effect of microstructure and rock mineralogy on water imbibition characteristics in tight reservoirs. *J. Nat. Gas Sci. Eng.* **2016**, *34*, 1461–1471. [CrossRef]
18. Tan, J.; Hu, C.; Lyu, Q.; Feng, G.; Chen, S. Experimental investigation on the effects of different fracturing fluids on shale surface morphology. *J. Pet. Sci. Eng.* **2022**, *212*, 110356. [CrossRef]
19. Taheri, A.; Zhang, Y.; Munoz, H. Performance of rock crack stress thresholds determination criteria and investigating strength and confining pressure effects. *Constr. Build. Mater.* **2020**, *243*, 118263. [CrossRef]
20. Wang, S.; Huang, R.; Ni, P.; Gamage, R.P.; Zhang, M. Fracture Behavior of Intact Rock Using Acoustic Emission: Experimental Observation and Realistic Modeling. *Geotech. Test. J.* **2013**, *36*, 20120086. [CrossRef]
21. Kong, R.; Feng, X.-T.; Zhang, X.; Yang, C. Study on crack initiation and damage stress in sandstone under true triaxial compression. *Int. J. Rock Mech. Min. Sci.* **2018**, *106*, 117–123. [CrossRef]
22. Li, C.; Xie, H.; Wang, J. Anisotropic characteristics of crack initiation and crack damage thresholds for shale. *Int. J. Rock Mech. Min. Sci.* **2020**, *126*, 104178. [CrossRef]
23. Yang, L.; Fan, C.; Wen, H.; Luo, M.; Sun, H.; Jia, C. An improved gas–liquid–solid coupling model with plastic failure for hydraulic flushing in gassy coal seam and application in borehole arrangement. *Phys. Fluids* **2023**, *35*, 036603. [CrossRef]
24. Tang, M.; Wang, G.; Chen, S.; Yang, C. Crack initiation stress of brittle rock with different porosities. *Bull. Eng. Geol. Environ.* **2021**, *80*, 4559–4574. [CrossRef]
25. Tang, M.; Wang, G.; Chen, S.; Yang, C. An Objective Crack Initiation Stress Identification Method for Brittle Rock Under Compression Using a Reference Line. *Rock Mech. Rock Eng.* **2021**, *54*, 4283–4298. [CrossRef]
26. Hu, Y.; Zhao, C.; Zhao, J.; Wang, Q.; Zhao, J.; Gao, D.; Fu, C. Mechanisms of fracturing fluid spontaneous imbibition behavior in shale reservoir: A review. *J. Nat. Gas Sci. Eng.* **2020**, *82*, 103498. [CrossRef]
27. Ündül, Ö.; Amann, F.; Aysal, N.; Plötze, M.L. Micro-textural effects on crack initiation and crack propagation of andesitic rocks. *Eng. Geol.* **2015**, *193*, 267–275. [CrossRef]
28. Martin, C.D.; Chandler, N.A. The progressive fracture of Lac du Bonnet granite. *Int. J. Rock Mech. Min. Sci. Geomech. Abstr.* **1994**, *31*, 643–659. [CrossRef]
29. Lajtai, E.Z.; Lajtai, V.N. The evolution of brittle fracture in rocks. *J. Geol. Soc.* **1974**, *130*, 1–16. [CrossRef]
30. Xia, X.; Li, H.; Li, J.; Liu, B.; Yu, C. A case study on rock damage prediction and control method for underground tunnels subjected to adjacent excavation blasting. *Tunn. Undergr. Space Technol.* **2013**, *35*, 1–7. [CrossRef]
31. Cai, M.; Kaiser, P.K.; Tasaka, Y.; Maejima, T.; Morioka, H.; Minami, M. Generalized crack initiation and crack damage stress thresholds of brittle rock masses near underground excavations. *Int. J. Rock Mech. Min. Sci.* **2004**, *41*, 833–847. [CrossRef]

32. Zhao, G.; Guo, Y.; Wang, L.; Chang, X.; Yang, H.; Guo, W.; Wu, X.; Yang, C. Experimental Study on Mechanical, Brittleness, and Fracture Behavior of Deep Shales Subjected to Fracturing Fluid-Shale Interactions at Reservoir Temperature and In-Situ Stress Conditions. *Rock Mech. Rock Eng.* **2023**, *56*, 1–18. [CrossRef]
33. Hua, G.; Wu, S.; Jing, Z.; Yu, X.; Xu, K.; Shi, W.; Guan, M. Rock physical and chemical alterations during the in-situ interaction between fracturing fluid and Silurian organic-rich shales in China. *J. Nat. Gas Sci. Eng.* **2021**, *94*, 104075. [CrossRef]